

Cite this: *Org. Biomol. Chem.*, 2011, **9**, 7016

www.rsc.org/obc

PAPER

Reactivity of *p*-nitrostyrene oxide as an alkylating agent. A kinetic approach to biomimetic conditions

Marina González-Pérez, Rafael Gómez-Bombarelli, M. Teresa Pérez-Prior, José A. Manso, Isaac F. Céspedes-Camacho, Emilio Calle and Julio Casado\*

Received 6th June 2011, Accepted 14th July 2011

DOI: 10.1039/c1ob05909b

The alkylating potential of *p*-nitrostyrene oxide (*p*NSO)—a compound used as a substrate to study the activity of epoxide hydrolases as well as in polymer production and in the pharmaceutical industry—was investigated kinetically. The molecule 4-(*p*-nitrobenzyl)pyridine (NBP), as a model nucleophile for DNA bases, was used as an alkylation substrate. In order to gain insight into the effect of the hydrolysis of *p*NSO, as well as the hydrolysis of the NBP-*p*NSO adduct on the *p*NSO alkylating efficiency, these two competing reactions were studied in parallel with the main NBP-alkylation reaction. The following conclusions were drawn: (i) *p*NSO reacts through an S<sub>N</sub>2 mechanism, with NBP to form an adduct, *p*NSO-NBP (AD). The rate equation for the adduct formation is:  $r = d[AD]/dt = k_{\text{alk}}[NBP][pNSO] - k_{\text{hyd}}^{\text{AD}}[AD]$  ( $k_{\text{alk}}$ , and  $k_{\text{hyd}}^{\text{AD}}$  being the alkylation rate constant and the NBP-*p*NSO adduct hydrolysis rate constant, respectively); (ii) the alkylating capacity of *p*NSO, defined as the fraction of initial alkylating agent that forms the adduct, is similar to that of mutagenic agents as effective as  $\beta$ -propiolactone. The instability of the *p*NSO-NBP adduct formed could be invoked to explain the lower mutagenicity shown by *p*NSO; (iii) the different stabilities of the  $\alpha$  and  $\beta$ -adducts formed between NBP and styrene oxides show that the alkylating capacity  $f = k_{\text{alk}}[NBP]/(k_{\text{alk}}[NBP] + k_{\text{hyd}})$  ( $k_{\text{hyd}}$  being the *p*NSO hydrolysis rate constant) as well as the alkylating effectiveness,  $AL = f/k_{\text{hyd}}^{\text{AD}}$ , are useful tools for correlating the chemical reactivity and mutagenicity of styrene oxides; (iv) a *p*NSO-guanosine adduct was detected.

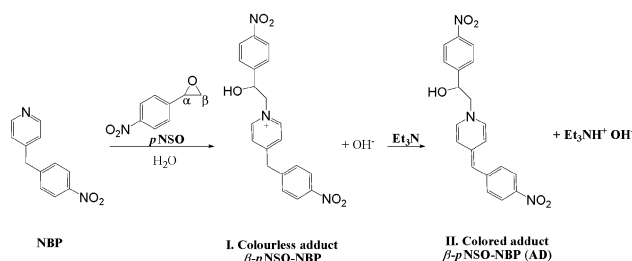
## Introduction

Substituted styrene oxides are extensively used in the pharmaceutical synthesis of antileukemic, antibacterial, antianginal and antiarrhythmic drugs<sup>1–5</sup> since they and their corresponding glycols afford chiral building blocks to be obtained that are useful in the synthesis of biologically active molecules. For such purposes, epoxide hydrolases are used as a cheap and available tool.<sup>6,7</sup> *p*-Nitrostyrene oxide (*p*NSO), used in the polymer industry as well as in the synthesis of compounds such as the antianginal and antiarrhythmic Nifenalol<sup>®</sup>,<sup>5,8,9</sup> is the main standard substrate used to investigate the mechanism of action of these enzymes, because of its slow rate of spontaneous hydrolysis.<sup>10–13</sup>

Since to our knowledge: i) the alkylating potential of *p*NSO has not been investigated in depth considering neither the stability of *p*NSO itself nor that of its adduct with the alkylation substrate, factors which should modulate the efficiency of *p*NSO as an alkylating agent; and ii) no clear correlation has been observed to date between the chemical reactivity and mutagenicity of styrene oxides,<sup>14–16</sup> here we were prompted to address these issues.

## Experimental

The NBP alkylation reaction by *p*NSO was monitored spectrophotometrically at  $\lambda = 560$  nm, where the adduct spectrum shows a maximum. Because of the insolubility of NBP in water, the alkylation reactions were performed in a 7 : 3 (vol.) water/dioxane medium. Aliquots of the alkylation mixture (2.4 ml) were added over time to a cuvette containing 0.6 ml of 99% triethylamine. The addition of the base stopped the alkylation reaction and generated a blue colour due to the deprotonation of the adduct (Scheme 1).

Scheme 1 Method for monitoring NBP alkylation by *p*NSO.

Acetate, phosphate and borate buffers were used to maintain pH constant in the 4–9 range.

Departamento de Química física, Universidad de Salamanca, E-37008, Salamanca, Spain. E-mail: jucali@usal.es; Fax: +34 923 294574; Tel: +34 923 294486

For each kinetic run of the *p*NSO hydrolysis reaction, 20  $\mu$ l of the stock solution (epoxide  $(2.4\text{--}4.8)\times 10^{-3}$  M in dioxane) was added to a cuvette containing 3.0 ml of thermostatted reaction mixture (water+HClO<sub>4</sub>+dioxane). The rate of *p*NSO hydrolysis was determined spectrophotometrically by monitoring absorbance at  $\lambda = 310$  nm. The reaction was followed until no change in absorbance was observed.

A Shimadzu LC20A system coupled with a Shimadzu SPD-M20A diode array detector was used to follow the kinetics of *p*NSO hydrolysis. Chromatographic separation was achieved on a Mediterranean Sea C18 column (25 mm  $\times$  1 mm, 5  $\mu$ m). Mobile phase A was acetate buffer (pH = 4.75 and 0.1 M) and mobile phase B was acetonitrile. 35% B was maintained for 5 min, after which a gradient up to 90% B was run over 10 min and later held for 20 min. The flow rate was set at 1 ml min<sup>-1</sup> and 200  $\mu$ l of the hydrolysis mixture was injected.

Computational calculations were carried out using Gaussian 03W. Energy barriers were obtained by optimization of the geometries of the reactants and transition states in the DFT-B3LYP/6-31++G(d,p) basis set and the structures were characterized by harmonic analysis. The IEFPCM model Self Consistent Reaction Field (SCRFF) with the default parameters was used in the solvation calculation.

Absorbance measurements were performed with a Shimadzu UV-2401 PC spectrophotometer with a thermoelectric six-cell holder temperature control system. Temperature was kept constant ( $\pm 0.05$  °C) with a Lauda Ecoline RE120 thermostat. For pH measurements, a Metrohm 827 pH-meter was used.

Negative and positive-mode electrospray ionization mass spectra were recorded on a Waters ZQ4000 spectrometer by direct injection.

All kinetic runs were performed in triplicate.

In order to study the formation of the *p*NSO-guanosine adduct, guanosine ( $9.6 \times 10^{-4}$  M) was treated with *p*NSO (1.1 mM) in 1 : 4 (vol.) dioxane/acetate buffer (0.02 M and pH 3.99) by incubation at 45 °C for 5 days. The reaction mixture was separated by HPLC. A gradient consisting of 20 mM ammonium formate, pH 4.6, (A) and acetonitrile (B) with a flow rate 0.2 ml min<sup>-1</sup> was used. Initial elution was 100% A, followed by an increase in the proportion of B to 50%, which was maintained for 5 min and increased to 100% in 1 min. Peak detection was carried out by UV-absorption with a diode array detector and by negative electrospray ionization mass spectrometry. An HPLC Waters Alliance 2795 equipped with a C-18 column was used (Atlantis 100  $\times$  2.1 mm, 3.5  $\mu$ m).

Water was deionized with a MilliQ-Gradient (Millipore). Guanosine (98%), (R)-*p*NSO (99%) and NBP were from Sigma–Aldrich (98%). Dioxane was from Panreac.

Numerical treatment of the data was performed using the 7.1.44 Data Fit (Oakdale Engineering) software.

The reaction conditions are specified in the captions of the Figures, Schemes and Tables.

## Results

### $\beta$ -adduct formation

The nucleophilic ring-opening reaction of substituted styrene oxides can proceed at two sites:  $\alpha$ -CH and  $\beta$ -CH<sub>2</sub> (Scheme 1). The ratio of products formed depends on different factors, such

**Table 1** Theoretical energy barriers for the reaction of pyridine with several epoxides

Epoxide	Addition	$\Delta E$ (kJ mol <sup>-1</sup> )
Styrene oxide	$\beta$	91.4
	$\alpha$	93.5
<i>p</i> -Nitrostyrene oxide	$\beta$	86.9
	$\alpha$	97.7
Propylene oxide	$\beta$	89.9
	$\alpha$	104.7
Butylene oxide	$\beta$	105.1

as the nucleophile, the substituent of the styrene oxide and the medium.<sup>17–19</sup>

It is known that a high  $\beta$ - to  $\alpha$ -adduct concentrations ratio results in the reaction of *p*NSO with nucleophiles<sup>20–23</sup> (this ratio increases to 91% when pyridine is used as a nucleophile.)<sup>14</sup>

The energy barriers between the reactants and the transition states for the reaction between pyridine and several epoxides were calculated and are reported in Table 1. In the reaction with NBP (a substituted pyridine), no evidence of  $\alpha$ -adduct formation was found according to analyses of the mass spectra and fragmentation patterns (Fig. 1a). The absorption spectra, as well as the kinetic profiles for adduct formation, are in agreement with these results (Fig. 1b).

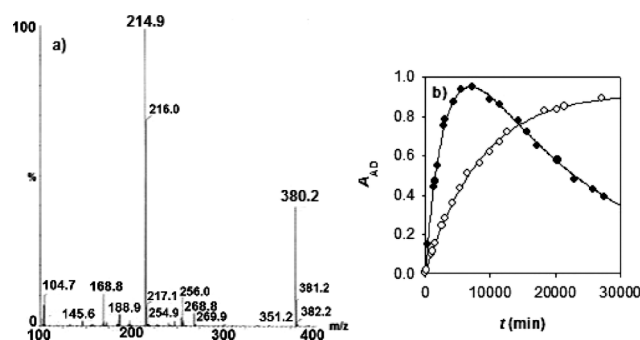


**Fig. 1** a) Positive-mode mass spectra obtained for the alkylation mixture after 10 days in NBP excess.  $T = 37.5$  °C; pH = 6.78; [NBP]<sub>0</sub> =  $1.56 \times 10^{-2}$  M; [*p*NSO]<sub>0</sub> =  $4.93 \times 10^{-5}$  M. b) Kinetic profiles obtained in 7 : 3 water/dioxane (vol) media with different acidities,  $T = 37.5$  °C;  $\lambda = 360$  nm; pH = 4.43; [NBP]<sub>0</sub> =  $1.29 \times 10^{-2}$  M (○); pH = 6.14; [NBP]<sub>0</sub> =  $1.56 \times 10^{-2}$  M (●).

Since the alkylation reaction of NBP by *p*NSO occurs in concurrence with the hydrolysis reactions of *p*NSO and of the  $\beta$ -NBP-*p*NSO adduct (AD) (Scheme 2), in the kinetic treatment of the NBP alkylation reaction it is necessary to take into account these side reactions.

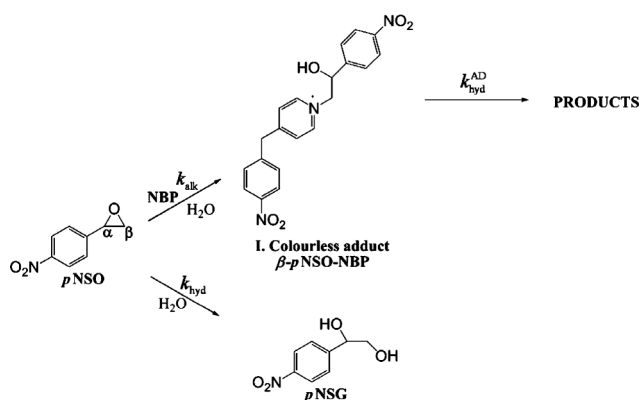
Since pH remains constant over time, the adduct formation rate can be expressed as

$$r = \frac{d[\text{AD}]}{dt} = k_{\text{alk}} [\text{NBP}] [\text{pNSO}] - k_{\text{hyd}}^{\text{AD}} [\text{AD}] \quad (1)$$

where  $k_{\text{alk}}$  is the NBP alkylation rate constant and  $k_{\text{hyd}}^{\text{AD}}$  is the hydrolysis rate constant of the adduct.

NBP was in large excess, such that its concentration was assumed to remain constant and a pseudo-first order rate constant was defined as  $k'_{\text{alk}} = k_{\text{alk}} [\text{NBP}]$ .

Eqn (2) gives the concentration of *p*NSO.



**Scheme 2** Reactions involved in the alkylation of NBP by *p*NSO.

$$[pNSO] = [pNSO]_0 e^{-(k'_{alk} + k_{hyd})t} \quad (2)$$

$[pNSO]_0$  being the initial concentration of *p*NSO and  $k_{hyd}$  the observed hydrolysis rate constant.

The absorbance of the adduct at time  $t$ ,  $A_{AD}$  (eqn (3)), was obtained by substitution of eqn (2) into eqn (1), subsequent integration and applying the Lambert–Beer law.

$$A_{AD} = \frac{k'_{alk} [pNSO]_0 \epsilon l}{(k'_{alk} + k_{hyd}) - k_{AD}} \left[ e^{-k_{AD}t} - e^{-(k'_{alk} + k_{hyd})t} \right] \quad (3)$$

$\epsilon$  being the adduct molar absorption coefficient, and  $l$  the cuvette light path.

Eqn (3) can be written in terms of three parameters:  $a$ ,  $b$ , and  $c$ , whose values can be obtained by non-linear optimization.

$$A_{AD} = \frac{a}{b - c} [e^{-ct} - e^{-bt}] \quad (4)$$

The observed kinetic profiles (Fig. 1b) show a good fit to eqn (4) and revealed that adduct hydrolysis in acid media ( $pH < 4.5$ ) can be considered negligible ( $c \sim 0$ ). The reaction orders with respect to  $[pNSO]$  and  $[NBP]$  ( $m$  and  $n$ , respectively; see eqn (5)) were determined with the Initial Rate Method (IRM).<sup>24</sup> Two series of experiments were carried out varying the concentration of each reactant. Fig. 2a shows that  $m = n = 1$ .

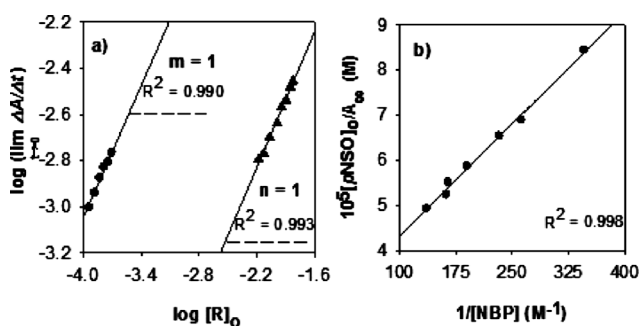


**Fig. 2** a) Reaction orders with respect to each reagent (R) (▲) NBP  $-[pNSO]_0 = 3.9 \times 10^{-4}$  M- and (●) *p*NSO  $-[NBP]_0 = 1.54 \times 10^{-2}$  M- in 7:3 water/dioxane;  $T = 37.5$  °C;  $pH = 6.97$ . b) Determination of the NBP-*p*NSO adduct molar absorption coefficient in 7:3 water/dioxane.  $T = 37.5$  °C;  $pH = 4.43$ ;  $[pNSO]_0 = 4.93 \times 10^{-5}$  M.

**Table 2** Rate constants and  $f$  values for the NBP alkylation reaction by *p*NSO as a function of temperature

$T/^\circ\text{C}$	$10^3 k_{alk} \text{ (M}^{-1} \text{ min}^{-1})^a$	$f$
30.0	$0.84 \pm 0.05$	0.92
32.5	$1.03 \pm 0.06$	0.87
35.0	$1.28 \pm 0.06$	0.85
37.5	$1.49 \pm 0.09$	0.84
40.0	$1.8 \pm 0.1$	0.84
42.5	$2.1 \pm 0.1$	0.83

<sup>a</sup>  $pH = 7.0$ . The relative error associated with  $f$  values is 10%.

$$v_o = \lim_{t \rightarrow 0} \frac{\Delta A}{\Delta t} = k_{alk} \epsilon l [NBP]_0^n [pNSO]_0^m \quad (5)$$

### Molar absorption coefficient of the NBP-*p*NSO adduct

Determination of the molar absorption coefficient of the adduct ( $\epsilon$ ) is of interest because it allows the NBP alkylation rate constant ( $k_{alk}$ ) to be determined simply by measuring measurement of the initial rate (eqn (5)).

At  $t = \infty$  and  $pH \leq 4.5$ , eqn (3) can be written as eqn (6):

$$\frac{[pNSO]_0}{A_\infty} = \frac{k_{hyd}}{k_{alk} \epsilon l [NBP]} + \frac{1}{\epsilon l} \quad (6)$$

Experiments performed at  $pH = 4.43$  afforded  $\epsilon = (3.7 \pm 0.2) \times 10^4 \text{ M}^{-1} \text{ cm}^{-1}$  (Fig. 2b).

### Alkylation rate constant

The  $k_{alk}$  values obtained by the IRM are in accordance with those resulting from parameter  $b$  (eqn (3)). No variations in  $k_{alk}$  values with  $pH$  were observed in the 4.5–9 range. A good fit of the  $k_{alk}$  values at different temperatures (Table 2) to the Arrhenius and Eyring–Wynne–Jones equations was found (eqn (7)).

$$\ln \frac{k}{T} = \frac{\Delta^\ddagger S^\circ}{R} + \ln \frac{k}{h} - \frac{\Delta^\ddagger H^\circ}{RT} \quad (7)$$

The activation parameters were obtained from the slope and intercept. They are similar to those obtained by Laird and Parker with *p*-bromo and *p*-methylstyrene oxides using benzylamine as a nucleophile (Table 3).<sup>20</sup>

**Table 3** Activation parameters for the  $S_N2$  alkylation and spontaneous hydrolysis reactions of several compounds

Reaction	Compound	$\Delta^\ddagger H^\circ \text{ (kJ mol}^{-1})$	$-\Delta^\ddagger S^\circ \text{ (J K}^{-1} \text{ mol}^{-1})$
Alkylation	<i>p</i> NSO <sup>a</sup>	$54 \pm 2$	$139 \pm 5$
	<i>p</i> -Bromostyrene oxide <sup>b</sup>	42.3	190
	<i>p</i> -Methylstyrene oxide <sup>b</sup>	54.9	157
Hydrolysis	<i>p</i> NSO <sup>a</sup>	$64 \pm 6$	$81 \pm 18$
	Ethylene oxide <sup>c,d</sup>	$79 \pm 8$	$99 \pm 25$
	Diketene <sup>e</sup>	$59 \pm 1$	$156 \pm 5$
	BPL <sup>e</sup>	$79 \pm 1$	$95 \pm 3$

Values taken from<sup>a</sup> This work. 7:3 water/dioxane medium;  $pH = 7$ ,  $[NBP]_0 = 1.49 \times 10^{-2}$  M. <sup>b</sup> Ref. 20. The nucleophile used was benzylamine. <sup>c</sup> Ref. 25. <sup>d</sup> Ref. 26. <sup>e</sup> Ref. 27.

**Table 4** *p*NSO Hydrolysis catalytic rate constant as a function of the composition of the medium;  $T = 37.5\text{ }^{\circ}\text{C}$ 

Water/dioxane (vol.)	Dielectric constant ( $\epsilon$ ) <sup>a</sup>	$k_{\text{H}^+}$ ( $\text{M}^{-1} \text{min}^{-1}$ )
10:0	74.0	$1.09 \pm 0.06$
9:1	65.5	$0.70 \pm 0.06$
8:2	57.1	$0.53 \pm 0.04$

<sup>a</sup> Values taken from ref. 29.

### Hydrolysis of *p*-nitrostyrene oxide

Since *p*NSO undergoes acid and base hydrolysis ( $\text{pH} < 4$  and  $\text{pH} > 12$ , respectively),<sup>28</sup> the hydrolysis rate constant is the sum of the spontaneous hydrolysis rate constant,  $k_{\text{hyd}}^{\circ} = k_{\text{H}_2\text{O}}[\text{H}_2\text{O}]$ , and the catalytic hydrolysis rate constants (eqn(8)):

$$k_{\text{hyd}} = k_{\text{hyd}}^{\circ} + k_{\text{H}^+} + k_{\text{OH}^-}[\text{OH}^-] \quad (8)$$

### Acid-catalyzed hydrolysis

The hydrolysis reaction in 7:3 (v/v) water/dioxane ( $\text{pH} = 3$ ) was followed by HPLC separation and UV detection. The evolution of the chromatograms over time and the kinetic profiles are corresponding to that of the glycol, appeared in the chromatograms (Fig. 3). The reaction kinetics was followed by monitoring ( $\lambda = 254 \text{ nm}$ ) the decrease in the *p*NSO peak area at a retention time of  $t_{\text{R}} = 28 \text{ min}$  (eqn (9)) as well as the increase in that of *p*NSG ( $t_{\text{R}} = 20 \text{ min}$ ) (eqn (10)) over time:

$$\text{Area}_{p\text{NSG}} = \text{Area}_{p\text{NSG}^{\circ}}(1 - e^{-k_{\text{hyd}}t}) \quad (9)$$

$$\text{Area}_{p\text{NSO}} = \text{Area}_{p\text{NSO}^{\circ}}e^{-k_{\text{hyd}}t} \quad (10)$$

Since in acid media the variation in absorbance along time in 7:3 water/dioxane is too small to be followed spectrophotometrically, and since the reaction rate ( $T = 37.5\text{ }^{\circ}\text{C}$ ) is too fast to be followed by HPLC separation and UV detection, the *p*NSO hydrolysis reaction rate constants were obtained indirectly.

The hydrolysis catalytic coefficient in 7:3 water/dioxane,  $k_{\text{H}^+} = (3.2 \pm 0.1) \times 10^{-1} \text{ M}^{-1} \text{min}^{-1}$  ( $T = 37.5\text{ }^{\circ}\text{C}$ ), was determined by extrapolation from its values in media with higher water ratios (Table 4).

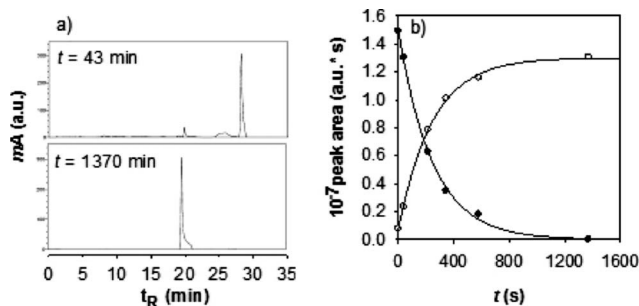


**Fig. 3** a) Chromatogram of the temporal evolution of acid-catalyzed hydrolysis,  $\lambda = 310 \text{ nm}$ . b) Kinetic profiles obtained by following peak area variation for *p*NSO and its hydrolysis product over time,  $\lambda = 254 \text{ nm}$ .  $T = 25.0\text{ }^{\circ}\text{C}$ ;  $\text{pH} = 2.99$ ;  $[p\text{NSO}]_0 = 4.93 \times 10^{-5} \text{ M}$ .

These values were obtained by direct spectrophotometry ( $\lambda = 310 \text{ nm}$ ). Absorbance ( $A$ ) at time  $t$  was the sum of the epoxide and the glycol contributions (eqn (11)).

$$A = [p\text{NSO}]_0[\epsilon_{p\text{NSG}} + (\epsilon_{p\text{NSO}} - \epsilon_{p\text{NSG}})e^{-k_{\text{hyd}}t}] \quad (11)$$

In strongly acidic media ( $\text{pH} \leq 2.6$ ;  $k_{\text{hyd}} = k_{\text{H}^+}[\text{H}^+]$ ), the catalytic constant  $k_{\text{H}^+}$  for each medium is given by the slope of the plot  $k_{\text{hyd}}/[\text{H}^+]$  (experiments performed for each medium at different pH-values revealed first order ( $\alpha = 1$ ) with respect to  $[\text{H}^+]$ ; see Fig. 4a).

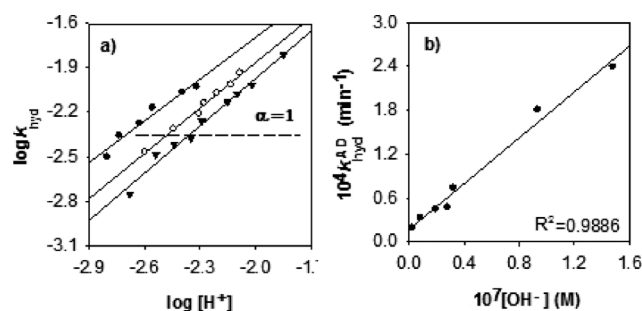


**Fig. 4** a) Variation in the *p*NSO hydrolysis rate constant with the acidity of the medium in water/dioxane media 10:0 (●), 9:1 (○) and 8:2 (▼);  $T = 37.5\text{ }^{\circ}\text{C}$ . b) Influence of  $[\text{OH}^-]$  on  $k_{\text{hyd}}^{\text{AD}}$ .

### Spontaneous hydrolysis reaction

The *p*NSO hydrolysis rate constant for the spontaneous reaction ( $k_{\text{hyd}} = k_{\text{hyd}}^{\circ}$ ;  $\text{pH} = 4.5\text{--}7$ ) was calculated from the parameter  $b$  of eqn (4), such that  $k_{\text{hyd}} = (6.3 \pm 0.6) \times 10^{-5} \text{ min}^{-1}$  ( $T = 37.5\text{ }^{\circ}\text{C}$ ). As a consequence, a value of  $k_{\text{H}_2\text{O}} = (1.6 \pm 0.2) \times 10^{-6} \text{ M}^{-1} \text{min}^{-1}$  ( $T = 37.5\text{ }^{\circ}\text{C}$ ;  $[\text{H}_2\text{O}] = 38.9 \text{ M}$ ) was obtained. Activation parameters were provided by the fit of  $k_{\text{hyd}}^{\circ}$  at different temperatures to the Arrhenius and Eyring-Wynne-Jones equations respectively (Table 3). The negative entropies of activation are consistent with a bimolecular nucleophilic substitution ( $\text{S}_{\text{N}}2$ -type mechanism), as expected for a styrene oxide with an electron-withdrawing substituent in the ring.<sup>17–21</sup>

### Efficiency of the *p*NSO as an alkylating agent

The alkylating capacity of *p*NSO can be defined as the fraction ( $f$ ) of initial *p*NSO forming the adduct (eqn (12)):

$$f = \frac{k_{\text{alk}}[\text{NBP}]}{(k_{\text{alk}}[\text{NBP}] + k_{\text{hyd}})} \quad (12)$$

The  $f$  values found at different temperatures and in media with different acidities are shown in Tables 2 and 5, respectively.

### Hydrolysis of NBP-*p*NSO adduct

The hydrolysis of the NBP-*p*NSO adduct is base-catalyzed (Fig. 4b). The values of the hydrolysis rate constants were calculated from the parameter  $c$  of eqn (4). Since eqn (13) gives

$$c = k_{\text{hyd}}^{\text{AD}} = k_{\text{hyd,OH}^-}^{\text{AD}}[\text{OH}^-] + k_{\text{hyd,o}}^{\text{AD}} \quad (13)$$



**Table 5** Influence of pH on  $f$  and AL;  $T = 37.5^\circ\text{C}$ 

pH	$f$	$10^3\text{AL (min)}$
4.50	0.73	216
4.97	0.76	72
5.42	0.77	39
5.91	0.75	22
6.11	0.74	15
6.29	0.86	19
7.17	0.84	3.5

[NBP] =  $1.49 \times 10^{-2}$  M. The errors associated with  $f$  and AL values are about 10%.

the slope and intercept of the  $k_{\text{hyd}}^{\text{AD}}/[\text{OH}^-]$  plot allow the values of  $k_{\text{hyd OH}^-}^{\text{AD}} = (1.53 \pm 0.07) \times 10^3 \text{ M}^{-1} \text{ min}^{-1}$  and  $k_{\text{hyd}}^{\text{AD}} = (2.2 \pm 0.5) \times 10^{-5} \text{ min}^{-1}$  to be determined.

## Discussion

The presence of the nitro group in the *para* position of styrene oxide governs the reactivity of *p*NSO. Whereas very little difference between the energy barriers for the  $\beta$ - and  $\alpha$ -transition states in the reaction with pyridine (Table 1) were obtained *in silico* for styrene oxide in the case of *p*-nitrostyrene oxide, this difference is as large as that due to propylene oxide (PO). The difference of  $\sim 10 \text{ kJ mol}^{-1}$  (*ca.* a hundred-fold decrease in the reaction rate) suggests that the attack on the  $\beta$ -position is favoured. This helps to understand the fact that alkylation reactions with SO usually yield a mixture of both adducts,<sup>19,30,31</sup> whereas PO only reacts through the  $\beta$  position<sup>31,32</sup> and it also suggests the negligible formation of an  $\alpha$ -adduct by *p*NSO. Several experimental findings have also shown that the NBP alkylation reaction by *p*NSO occurs through the  $\beta$  position.

The activation parameters and the reaction orders revealed that spontaneous *p*NSO hydrolysis and alkylation reactions occur through  $\text{S}_{\text{N}}2$  mechanisms, respectively, as expected. The reaction between styrene oxide and guanosine at position N7 also takes place through this mechanism.<sup>33</sup> In the pH 4.5–7 range, these reactions are not influenced by the acidity of the medium (Fig. 5) and, consequently, neither is the alkylating capacity of *p*NSO:  $f$ . The value of this parameter, only slightly influenced by temperature, (Table 2), indicates that under all the conditions studied 80–90% of the initial amount of *p*NSO participated in the alkylation reaction, which points to the strong alkylating capacity of *p*NSO. It should be noted that *p*NSO is a strong alkylating agent, whose  $f$  value for NBP alkylation reaction is similar to

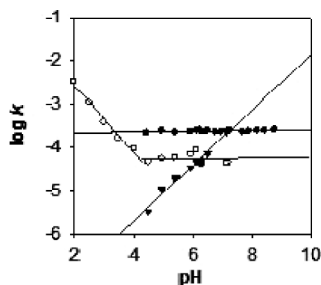


**Fig. 5** Influence of acidity on the reactions in the NBP alkylation reaction by *p*NSO in a 7 : 3 water/dioxane medium: (●)  $k_{\text{alk}}$ , (○)  $k_{\text{hyd}}$ , (▼)  $k_{\text{hyd}}^{\text{AD}}$ ;  $T = 37.5^\circ\text{C}$ ; [NBP]<sub>0</sub> =  $1.56 \times 10^{-2}$  M.

**Table 6** Alkylating capacity of *p*NSO compared with that of other alkylating agents

Alkylating agent	$f$	Mutagenicity <sup>g</sup>	LD <sub>50</sub> (M) <sup>h</sup>
$\beta$ -Propiolactone <sup>a</sup>	0.76	4.5	
$\beta$ -Butyrolactone <sup>a</sup>	0.62	n.a.	
Alkyldiazonium ions <sup>b</sup>	0.6–0.9	0.32–11	
Diketene <sup>c</sup>	1	~ 0	
Acetonitrile oxide <sup>d</sup>	0.13		
<i>p</i> -Nitrostyrene oxide <sup>e</sup>	0.82		$2.00 \times 10^{-3}$
Styrene oxide <sup>f</sup>	( $\beta$ ) 0.55 ( $\alpha$ ) 0.06	0.22	$5.70 \times 10^{-3}$

7 : 3 water/dioxane medium, [NBP]<sub>0</sub> =  $2.0 \times 10^{-2}$  M. <sup>a</sup> Values taken from ref. 34. <sup>b</sup> Ref. 35. <sup>c</sup> Ref. 27. <sup>d</sup> Ref. 36.  $T = 35.0^\circ\text{C}$ . <sup>e</sup> This work; pH = 7.17;  $T = 37.5^\circ\text{C}$ . <sup>f</sup> Unpublished. pH = 6.99;  $T = 37.5^\circ\text{C}$ . <sup>g</sup> Ref. 37. Values expressed as the increase in the number of 6-thioguanine-resistant mutants per  $10^6$  viable cells over the control values per  $\mu\text{g ml}^{-1}$ . <sup>h</sup> Ref. 14 Mutagenicity in *Salmonella typhimurium* TA100.

that of  $\beta$ -propiolactone: the most carcinogenic lactone (BPL, see Table 6).<sup>34</sup>

Unlike that lactone, *p*NSO forms an unstable adduct with the alkylation substrate. This makes it necessary to evaluate the net effectiveness of *p*NSO as an alkylating agent; that is, to take into account the adduct hydrolysis reaction, of the same order of magnitude as the alkylation reaction at cellular pH (Fig. 5). To do so, we defined adduct life (AL) as the total amount of adduct present along the progress of the reaction per unit of alkylating agent concentration, such that (eqn (14)):

$$\text{AL} = \frac{\int_0^\infty [\text{AD}] dt}{[\text{pNSO}]_0} = \frac{k'_{\text{alk}}}{k'_{\text{alk}} + k_{\text{hyd}} - k_{\text{hyd}}^{\text{AD}}} \int_0^\infty \left( e^{-(k'_{\text{alk}} + k_{\text{hyd}})t} - e^{-k_{\text{hyd}}^{\text{AD}}t} \right) dt$$

$$= \frac{k'_{\text{alk}}}{(k'_{\text{alk}} + k_{\text{hyd}})k_{\text{hyd}}^{\text{AD}}} = \frac{f}{k_{\text{hyd}}^{\text{AD}}} \quad (14)$$

NBP-*p*NSO adduct hydrolysis varies over two orders of magnitude from pH 4.5 to 7, reducing the NBP-*p*NSO adduct life considerably from 150 days to 55 h (Table 5). In spite of this alkylating capacity, the effectiveness of *p*NSO as an alkylating agent is low in comparison with that of other alkylating agents investigated previously.<sup>36</sup>

The results provided by previous studies<sup>14,16,38,39</sup> focused on the search for a correlation between the alkylating capacity and chemical reactivity of styrene oxides indicated that the mutagenic effect of styrene oxides depends on the structure of the adducts, but is not correlated with the amount of them formed. In some of these works, it was suggested that mutagenicity would only be correlated with the reactivity on the benzylic side, with  $\alpha$ -adduct formation.<sup>14,38,40</sup> Since styrene oxides that form only  $\beta$ -adducts, such as *p*NSO or  $\alpha$ -methylstyrene oxide derivatives, have also been shown to have mutagenic activity,<sup>14,41</sup> these explanations are not totally satisfactory. According to our results, such findings could be explained (Table 6) in terms of the high stability of  $\alpha$ -adducts, which should provide a greater—but not exclusive—contribution to carcinogenicity than unstable  $\beta$ -adducts. The longer the persistence of adducts over time, the higher the probability that mutagenic effects will appear. Since for several compounds a lack of carcinogenicity has previously been shown to

be correlated with the stability and instability of the corresponding adducts,  $f$  and AL could help to find a correlation between the reactivity and biological activity of styrene oxides.

The mutagenicity shown by  $\text{BPL} > p\text{NSO} > \text{SO}$  could be explained in these terms (Table 6). The higher the ratio and stability of the adduct formed, the higher the mutagenicity.

### Final remarks: $p\text{NSO}$ -guanosine adduct formation

Since, stated above, NBP is a model nucleophile for the N7 position of guanine in DNA,<sup>42–45</sup> the efficiency of  $p\text{NSO}$  as an alkylating agent of NBP has been investigated,<sup>46</sup> the last step of the present work was to check the  $p\text{NSO}$  alkylating capacity on a biomimetic substrate such as the guanosine molecule (Guo). This is in contrast with a previous work,<sup>15</sup> in which no evidence of its formation was found. The mass spectra of the aliquots eluted at a retention time of 8.83 min revealed the formation of a  $p\text{NSO}$ -guanosine adduct in the reaction of guanosine and  $p\text{NSO}$  (Fig. 6). This is in contrast with the results from earlier work,<sup>15</sup> in which no evidence of its formation was found. Currently, experiments to investigate in depth the formation mechanism of the  $p\text{NSO}$ -Guo adduct are being carried out.

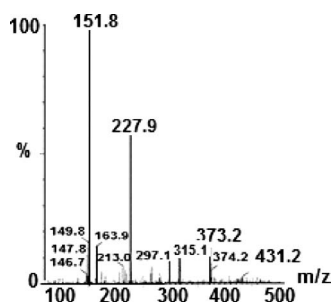


Fig. 6 Mass spectra of the peak with  $t_R = 8.83$  min from the chromatogram of  $p\text{NSO}$  and the guanosine reaction mixture.

### Conclusions

(i)  $p\text{NSO}$  alkylates 4-( $p$ -nitrobenzyl)pyridine (NBP), a model molecule of the N7 position of guanine in DNA, through an  $\text{S}_\text{N}2$  mechanism to form the  $\beta$ -NBP- $p\text{NSO}$  adduct (AD).

(ii) To study alkylating effectiveness, three reactions must be taken into account: a) The alkylation reaction itself; b) the  $p\text{NSO}$  hydrolysis reaction, which also occurs through an  $\text{S}_\text{N}2$  mechanism, and c) the  $p\text{NSO}$ -NBP adduct hydrolysis reaction.

(iii)  $p\text{NSO}$  is a strong alkylating agent but with low effectiveness. The alkylating capacity of  $p\text{NSO}$ , defined as the fraction of initial alkylating agent that forms the adduct, is similar to that of mutagenic agents as effective as  $\beta$ -propiolactone. The instability of the  $\beta$ -adduct formed that reduces its effectiveness could account for the low mutagenicity of  $p\text{NSO}$  in comparison with that seen for the lactone.

(iv) The different stabilities of the  $\alpha$  and  $\beta$ -adducts formed between NBP and styrene oxides show that the alkylating capacity,  $f = k_{\text{alk}}[\text{NBP}] / (k_{\text{alk}}[\text{NBP}] + k_{\text{hyd}})$ , as well as the alkylating effectiveness,  $\text{AL} = f / k_{\text{hyd}}^{\text{AD}}$  ( $k_{\text{alk}}$ ,  $k_{\text{hyd}}$  and  $k_{\text{hyd}}^{\text{AD}}$  being the alkylation rate constant, the  $p\text{NSO}$  hydrolysis rate constant, and the NBP- $p\text{NSO}$  adduct hydrolysis rate constant) are useful tools for

correlating the chemical reactivity and mutagenicity of styrene oxides.

(v) A  $p\text{NSO}$ -guanosine adduct was detected.

### Acknowledgements

We thank the Spanish Ministerio de Ciencia e Innovación and Fondos FEDER (Project CTQ2010-18999) for supporting the research reported in this article. M.G.P. thanks the Junta de Castilla y León for Ph. D. grant. R.G.B. thanks the Spanish Ministerio de Educación, and I.F.C. the Spanish Ministerio de Asuntos Exteriores y de Cooperación (MAEC-AECI Grant) for PhD grants.

### Notes and references

- Solladié-Cavallo and A. Diep-Vohuile, *J. Org. Chem.*, 1995, **60**, 3494.
- K. Hattori, M. Nagano, T. Kato, I. Nakanishi, I. Keisuke, T. Kinoshita and K. Sakane, *Bioorg. Med. Chem. Lett.*, 1995, **5**, 2821.
- R. Di Fabio, C. Pietra, R. J. Thomas and L. Ziviani, *Bioorg. Med. Chem. Lett.*, 1995, **5**, 551.
- R. K. Atkins, J. Frazier, L. L. Moore and L. O. Weigel, *Tetrahedron Lett.*, 1986, **27**, 2451.
- S. Pedragosa-Moreau, C. Morisseau, J. Baratti, J. Zylber, A. Archelas and R. Furstoss, *Tetrahedron*, 1997, **53**, 9707.
- S. Pedragosa-Moreau, J. Morisseau, J. Zylber, A. Archelas and R. Furstoss, *J. Org. Chem.*, 1996, **61**, 7402.
- N. Bala and S. S. Chimni, *Tetrahedron: Asymmetry*, 2010, **21**, 2879.
- H. Nellaiah, C. Morisseau, A. Archelas, R. Furstoss and J. C. Baratti, *Biotechnol. Bioeng.*, 1996, **49**, 70.
- A. O. Kas'yan, E. A. Golodaeva, A. V. Tsygankov, L. I. Kas'yan and Russ, *J. Org. Chem.*, 2002, **38**, 1606.
- R. B. Westkaemper and R. P. Hanzlik, *Anal. Biochem.*, 1980, **102**, 63.
- R. B. Westkaemper and R. P. Hanzlik, *Arch. Biochem. Biophys.*, 1981, **208**, 195.
- P. Moussou, A. Archelas, J. Baratti and R. Furstoss, *J. Org. Chem.*, 1998, **63**, 3532.
- C. A. Yeates, M. S. van Dyk, A. L. Botes, J. C. Breytenbach and H. M. Krieg, *Biotechnol. Lett.*, 2003, **25**, 675.
- N. Tamura, K. Takahashi, N. Shirai and Y. Kawazoe, *Chem Pharm. Bull.*, 1982, **30**, 1393.
- K. Hemminki, T. Heinonen and H. Vainio, *Arch. Toxicol.*, 1981, **49**, 35.
- K. Sugiura, T. Kimura and M. Goto, *Mutat. Res., Genet. Toxicol.*, 1978, **58**, 159.
- Y. Kawazoe, N. Tamura and T. Yoshimura, *Chem. Pharm. Bull.*, 1982, **30**, 2077.
- M. M. Kayser and P. Morand, *Can. J. Chem.*, 1980, **58**, 302.
- R. E. Parker and N. S. Isaacs, *Chem. Rev.*, 1959, **59**, 737.
- R. M. Laird and R. E. Parker, *J. Am. Chem. Soc.*, 1961, **83**, 4277.
- J. J. Blummenstein, V. C. Ukachukwu, R. S. Mohan and D. L. Whalen, *J. Org. Chem.*, 1993, **58**, 924.
- T. M. Santosusso and D. Swern, *J. Org. Chem.*, 1975, **40**, 2764.
- C. O. Guss and H. G. Mautner, *J. Org. Chem.*, 1951, **16**, 887.
- J. Casado, M. A. López-Quintela and F. M. Lorenzo-Barral, *J. Chem. Educ.*, 1986, **63**, 450.
- A. L. Mori and L. L. Schaleger, *J. Am. Chem. Soc.*, 1972, **94**, 5039.
- J. Koskikallio and E. Whalley, *Can. J. Chem.*, 1959, **37**, 783.
- R. Gómez-Bombarelli, M. González-Pérez, M. T. Pérez Prior, J. A. Manso, E. Calle and J. Casado, *Chem. Res. Toxicol.*, 2008, **21**, 1964.
- V. Gold, *Advances in physical organic chemistry* (Elsevier, New York, 1963).
- G. Akerlof and O. A. Sort, *J. Am. Chem. Soc.*, 1936, **58**, 1241.
- F. Latif, R. C. Moschel, K. Hemminki and A. Dipple, *Chem. Res. Toxicol.*, 1988, **1**, 364.
- W. Pauwels and H. Veulemans, *Mutat. Res., Genet. Toxicol. Environ. Mutagen.*, 1998, **418**, 21.
- L. Ehrenberg and S. Hussain, *Mutat. Res., Rev. Genet. Toxicol.*, 1981, **86**, 1.

- 33 T. Barlow and A. Dipple, *Chem. Res. Toxicol.*, 1998, **11**, 44.
- 34 J. A. Manso, M. T. Pérez-Prior, M. P. García-Santos, E. Calle and J. Casado, *Chem. Res. Toxicol.*, 2005, **18**, 1161.
- 35 J. A. Manso, M. T. Pérez-Prior, M. P. García-Santos, E. Calle and J. Casado, *J. Phys. Org. Chem.*, 2008, **21**, 932.
- 36 M. T. Pérez Prior, R. Gómez-Bombarelli, M. González-Pérez, J. A. Manso, M. P. García-Santos, E. Calle and J. Casado, *Chem. Res. Toxicol.*, 2009, **22**, 1320.
- 37 Y. Nishi, M. M. Hasegawa, M. Taketomi, Y. Ohkawa and N. Inui, *Cancer Res.*, 1984, **44**, 3270.
- 38 K. Sugiura and M. Goto, *Chem.-Biol. Interact.*, 1981, **35**, 71.
- 39 K. Hemminki and K. Falck, *Toxicol. Lett.*, 1979, **4**, 103.
- 40 K. Sugiura, Y. Shigeko, S. Fukasawa and M. Goto, *Chemosphere*, 1978, **9**, 737.
- 41 L. B. Rosman, V. G. Beylin, V. Gaddamidi, B. H. Hooberman and J. E. Sinsheimer, *Mutat. Res., Genet. Toxicol.*, 1986, **171**, 63.
- 42 K. Savela, A. Hesso and K. Hemminki, *Chem.-Biol. Interact.*, 1986, **60**, 235.
- 43 T. Barlow and A. Dipple, *Chem. Res. Toxicol.*, 1998, **11**, 44.
- 44 B. L. Van Duuren, L. Langseth, B. M. Goldschmidt and L. Orris, *J. Nat. Cancer Inst.*, 1967, **39**, 1217.
- 45 J. H. Kim and J. J. Thomas, *Bull. Environ. Contam. Toxicol.*, 1992, **49**, 879.
- 46 H. Norppa and H. Vainio, *Mutat. Res., Genet. Toxicol.*, 1983, **116**, 379.